

## Enhanced optical absorption due to $E_+$ -related band transition in GaAs:N $\delta$ -doped superlattices

Shuhei Yagi<sup>1\*</sup>, Shunsuke Noguchi<sup>1</sup>, Yasuto Hijikata<sup>1</sup>, Shigeyuki Kuboya<sup>2</sup>, Kentaro Onabe<sup>3</sup>, Yoshitaka Okada<sup>4</sup>, and Hiroyuki Yaguchi<sup>1</sup>

<sup>1</sup>Graduate School of Science and Engineering, Saitama University, Saitama 338-8570, Japan

<sup>2</sup>Institute for Materials Research, Tohoku University, Sendai 980-8577, Japan

<sup>3</sup>Department of Advanced Materials Science, The University of Tokyo, Kashiwa, Chiba 277-8561, Japan

<sup>4</sup>Research Center for Advanced Science and Technology, The University of Tokyo, Meguro, Tokyo 153-8904, Japan

E-mail: yagi@opt.ees.saitama-u.ac.jp

Received July 15, 2014; accepted September 8, 2014; published online September 26, 2014

The photoabsorption characteristics of GaAs:N  $\delta$ -doped superlattices (SLs) are investigated. Periodic insertion of N  $\delta$ -doped layers into GaAs induces the formation of conduction subbands  $E_+$  and  $E_-$ , and each conduction subband forms SL minibands with the GaAs conduction band between the  $\delta$ -doped layers. In addition to an optical absorption related to the  $E_-$  band, an abrupt absorption edge originating from the electron transition between the valence band and an  $E_+$ -related miniband is observed at 1.6 eV in a photoluminescence excitation (PLE) spectrum, indicating that GaAs:N  $\delta$ -doped SLs are promising candidates for the absorber of intermediate-band solar cells.

© 2014 The Japan Society of Applied Physics

GaAsN alloys containing up to a few percent of N have attracted attention as an intermediate-band absorber material for use in high-efficiency intermediate-band solar cells (IBSCs).<sup>1–5</sup> N incorporation in GaAs leads to the splitting of the conduction band (CB) into two subbands  $E_+$  and  $E_-$ . These conduction subbands and valence band (VB) are considered to compose an intermediate-band structure. To date, the observation of the upper conduction subband  $E_+$  in dilute nitride semiconductors has been mainly performed by reflection-based modulation spectroscopy such as photoreflectance (PR) and electroreflectance (ER).<sup>6–10</sup> From the viewpoint of application to IBSC absorbers, direct investigation of the absorption properties by transmission spectrophotometry or photoluminescence excitation (PLE) spectroscopy should be more important than that by reflection-based techniques. However, available reports on the direct observation of a distinct optical absorption edge originating from the  $E_+$  band by such absorption-based techniques are very limited. Although Skierbiszewski and co-workers showed absorption spectra of InGaAsN,<sup>11,12</sup> only a modest step associated with the  $E_+$  band absorption was detected in the spectra. In addition, a relatively elaborate process was required to prepare free-standing InGaAsN layers used for the measurements. The difficulty of detecting the  $E_+$  band absorption arises from the small oscillator strength of the  $E_+$  band transition, as indicated by the fact that the PR signal intensity of the  $E_+$  transition is generally much smaller than that of the  $E_-$  transition.<sup>6–10</sup> Furthermore, the optical absorption by thick GaAs substrates obscures the spectra of dilute nitride thin films in the energy range higher than the GaAs bandgap and makes it difficult to observe the  $E_+$  absorption characteristics.

The N  $\delta$ -doping technique is often used to explore new aspects of N-induced effects.<sup>13–17</sup> Recently, we proposed the use of superlattice (SL) structures consisting of N  $\delta$ -doped GaAs and undoped GaAs spacer layers for IBSCs as alternatives to the homogeneously N-doped GaAsN as an intermediate-band material because of their excellent optical properties.<sup>18,19</sup> We have demonstrated that, the PR transition signals associated with the  $E_+$  band are strongly enhanced for the SL structures compared with those for the conventional GaAsN alloys. In this study, we investigate the absorption

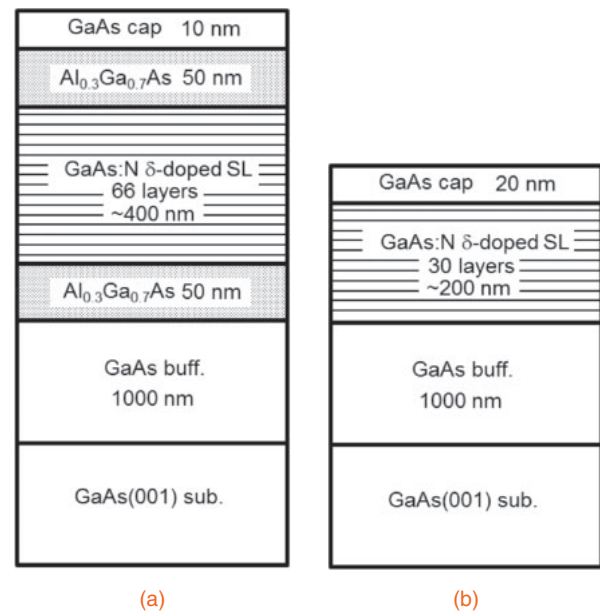


Fig. 1. Schematic illustrations of the fabricated samples: (a) sample A and (b) sample B.

properties of such GaAs:N  $\delta$ -doped SLs using PLE, and demonstrate a direct observation of a sharp optical absorption edge originating from the electron transitions associated with the N-induced  $E_+$  band in the SL structure.

The samples used in this study were grown on GaAs(001) substrates by metalorganic vapor phase epitaxy. Trimethylgallium (TMG), trimethylaluminum, tertiarybutylarsine, and dimethylhydrazine (DMHy) were used as the Ga, Al, As, and N sources, respectively. A GaAs buffer layer of 1000 nm thickness was grown on a substrate at 650 °C before the fabrication of N  $\delta$ -doped GaAs SLs. We fabricated two types of SL sample, the structures of which are schematically shown in Fig. 1. That is, one has two 50-nm-thick AlGaAs layers with an Al composition of 0.3, which sandwich 66 pairs of GaAs spacer/N  $\delta$ -doped layers (sample A); the other is with 30 pairs of GaAs spacer/N  $\delta$ -doped layers (sample B). N  $\delta$ -doped layers were formed by supplying DMHy on the growing surface while the TMG supply was

**Table I.** Structural parameters of GaAs:N  $\delta$ -doped SLs prepared in this study.

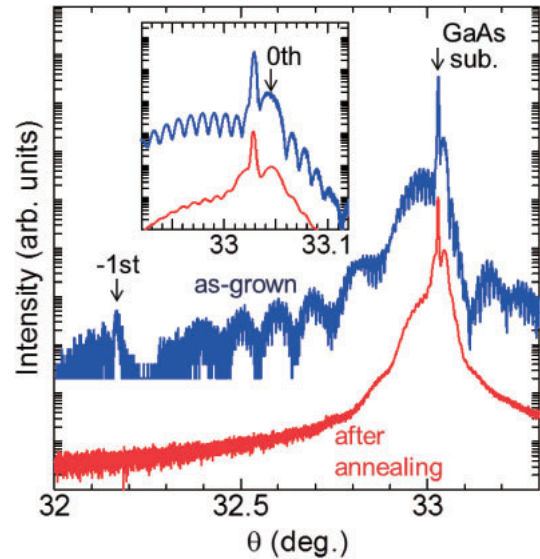
	Number of N $\delta$ -doping layers	SL period (nm)	N area density in a $\delta$ -doping layer ( $\text{cm}^{-2}$ )	Average N content in SL (%)
Sample A	66	6.0	$1.5 \times 10^{13}$	0.11
Sample B	30	6.9	$2.4 \times 10^{13}$	0.15

stopped. The SLs were fabricated by alternately forming a  $\delta$ -doped layer and a GaAs spacer layer. Both samples were capped by a thin GaAs layer. The structural parameters of the SLs, such as the N area density in a  $\delta$ -doped layer, the SL period (almost equivalent to the GaAs spacer thickness), and the average N concentration estimated by secondary ion mass spectroscopy or from X-ray diffraction (XRD), are summarized in Table I. We also prepared an annealed piece of sample A. The thermal annealing was carried out at 1000 °C for 5 min in N<sub>2</sub> atmosphere. The annealed sample was covered with a GaAs wafer to prevent As desorption during the annealing.

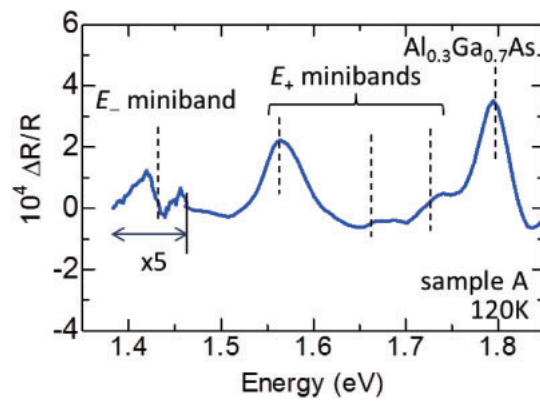
The energy structures and optical properties of the N  $\delta$ -doped SLs were investigated by PR, photoluminescence (PL), and PLE spectroscopies. In the PR measurements, a diode-pumped solid-state (DPSS) laser at 532 nm was used as a modulation light. The monochromatic probe light was obtained from a halogen lamp dispersed through a monochromator. PR signals were detected with a Si photodiode using a phase-sensitive lock-in amplification system. PL spectra were measured using a Ti-sapphire laser emitting at 720 nm as excitation light. PLE measurements were carried out by detecting PL while the excitation wavelength was scanned.

Figure 2 shows XRD patterns of sample A before and after annealing, as measured by  $\theta/2\theta$  scan. In addition to the 0th-order peak from the SL at the high-angle side of the GaAs(004) diffraction peak, the 1st-order satellite peak is clearly detected at 32.17° for the as-grown sample, verifying the periodic insertion of the N  $\delta$ -doped layers. The 1st-order SL satellite peak disappeared after annealing. This indicates the destruction of the periodic structure owing to the diffusion of N atoms. Note that the XRD peak from the N-containing layer of the annealed sample remains at the same angle of the 0th SL peak of the as-grown sample. Thus, out-diffusion of N to AlGaAs layers was negligible, and the average N content in the N-containing layer was maintained after annealing.

Figure 3 shows a PR spectrum of sample A in the as-grown state measured at 120 K. Energy positions of optical transitions estimated by fitting the spectrum with the Aspnes third-derivative functional form<sup>20)</sup> are indicated by dotted lines in the figure. The transition observed at 1.80 eV is attributed to the fundamental transition in the AlGaAs layers. In addition to the transition associated with the  $E_-$  band at 1.43 eV, several PR signals are observed in the energy range from 1.55 to 1.75 eV, in which no transitions are generally observed for homogeneously N-doped GaAsN alloys with N concentration comparable to the average N concentration of the SL. These transition energies can be interpreted by taking into account the SL potentials consisting of the CB of the GaAs spacer layers and modulated CBs around the N  $\delta$ -doped layers.<sup>18,19)</sup> The energy structure of a GaAs:N  $\delta$ -doped



**Fig. 2.** XRD patterns of sample A in the as-grown and annealed states. The annealing was carried out at 1000 °C for 5 min in N<sub>2</sub> atmosphere. The inset shows a magnified view of the patterns around the GaAs(004) peak.



**Fig. 3.** PR spectrum of sample A measured at 120 K. The vertical dotted lines indicate transition energies estimated by fitting.

SL is schematically shown in Fig. 4. The N-induced  $E_+$  and  $E_-$  bands are formed in the vicinity of a N  $\delta$ -doped layer, i.e., GaAs in the region behaves as a thin GaAsN layer. These modified CBs contribute to the formation of multiple SL minibands with the GaAs CB between the  $\delta$ -doped regions. The  $E_+$  band around the  $\delta$ -doped layers and GaAs CB act as the barrier and the well, respectively, resulting in minibands formed above the GaAs CB edge. Therefore, the PR signals at the high-energy side of the GaAs bandgap energy are attributed to transitions associated with the minibands in the  $E_+$  band/GaAs CB SL potential, whereas the PR signal at the low-energy side is due to a miniband in the  $E_-$  band (well)/GaAs CB (barrier) SL potential.

Figure 5 shows PL and PLE spectra of the GaAs:N  $\delta$ -doped SLs of samples A and B measured at 19 K. A spectrum of sample A after the thermal annealing is also shown in the figure. Emissions originating from GaAs band-edge and incorporated N-related states are observed at approximately 1.5 and 1.3–1.45 eV, respectively, in all the PL spectra. The intensity of the GaAs band-edge emission of sample B is much weaker than that of sample A. This can be understood

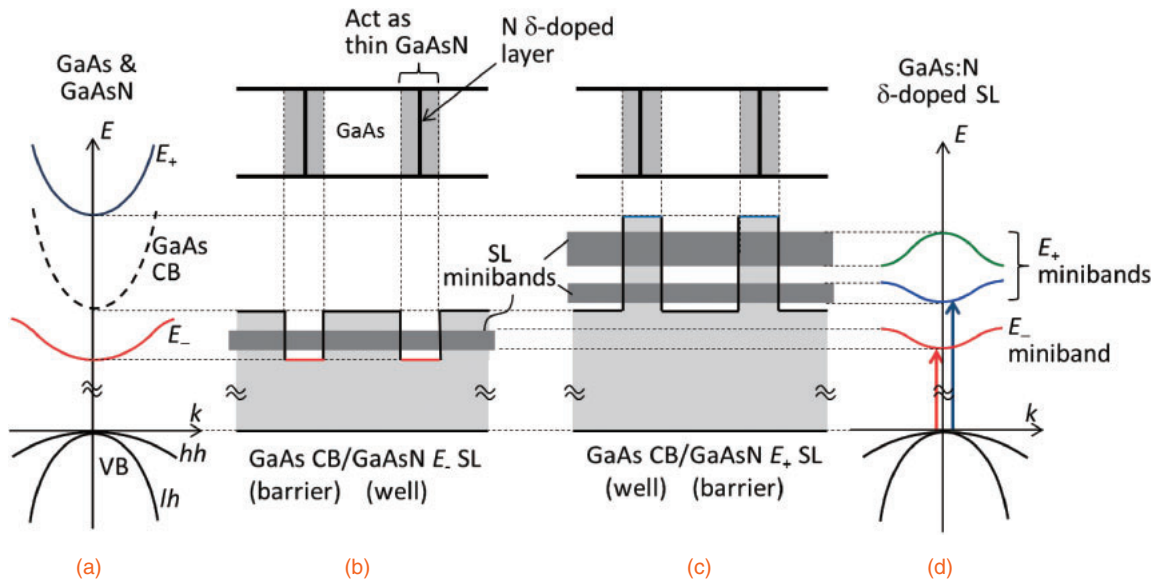


**Fig. 4.** Energy structure of GaAs:N  $\delta$ -doped SL. Energy dispersion relations of (a) GaAs and GaAsN (these are superposed) and (d) GaAs:N  $\delta$ -doped SL. (b) and (c) depict the  $E_-$  band/GaAs CB and  $E_+$  band/GaAs CB SL potentials, respectively. The optical transition pathways from the VB top to the  $E_+$  and  $E_-$  miniband bottoms are also depicted by vertical arrows in (d), which correspond to the absorption edges observed in PLE spectra in Fig. 5.

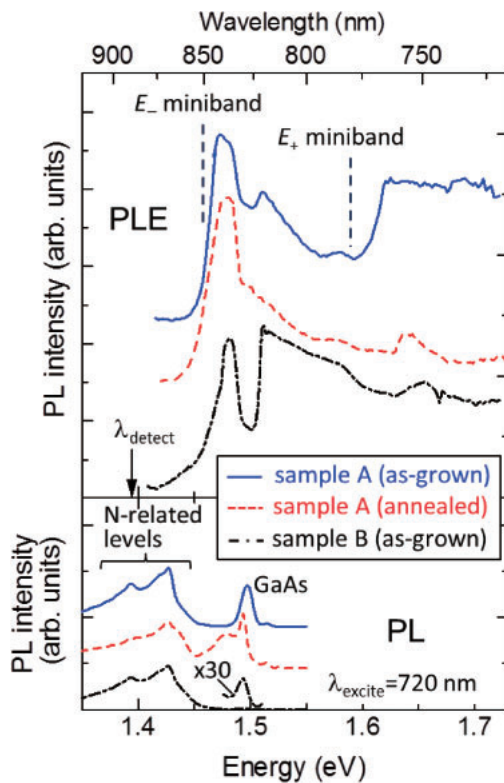


**Fig. 5.** PL and PLE spectra of the GaAs:N  $\delta$ -doped SLs measured at 19 K. The vertical dotted lines indicate transition energies associated with SL minibands for sample A in the as-grown state estimated by PR.

as follows. Carriers optically generated in the GaAs cap, buffer layer, and substrate of sample B diffuse into the SL region, which leads to the dominant emission from N-related levels because these levels are energetically lower than the GaAs CB. On the other hand, those carriers in sample A are blocked by the AlGaAs layers on both sides of the SL region, and thus they mainly recombine in the GaAs regions, resulting in the intense GaAs band-edge emission.

The PLE spectra were measured in an excitation energy range of 1.42–1.72 eV by detecting PL from a N-related state at 1.39 eV. Energy positions of the  $E_+$  and  $E_-$  miniband bottoms from the VB top estimated from the PR spectrum of sample A are indicated by vertical dotted lines in the figure. These energy positions are shifted by 23 meV to an energy higher than the PR transition energies because the difference in the measurement temperature between the PR and PLE measurements is taken into account. For both the as-grown samples, an absorption edge is observed at approximately 1.45 eV, which is attributed to the  $E_-$ -related miniband. In addition, a strong onset of the optical absorption is observed at about 1.6 eV only in the PLE spectrum of sample A in the as-grown state. This energy is in good agreement with the transition energy between the VB top and the lowest  $E_+$ -related miniband bottom estimated by the PR measurement. As mentioned, in sample B, most of the photocarriers generated in the GaAs cap, buffer, and substrate diffuse into the SL region and lead to photoemission from N-related states. Because these carriers affect the photoemission at the detected energy of 1.39 eV, the PLE spectrum strongly reflects the absorption properties of GaAs. Therefore, PLE signals from the SL should be obscured by that from the GaAs regions for sample B. On the other hand, photocarriers from the GaAs region of sample A are blocked by the AlGaAs layers located on both sides of the SL region. Thus, the effect of GaAs photoabsorption on the PLE spectrum is excluded for sample A, resulting in the successful detection of the absorption properties of the SL. This interpretation is also supported by the fact that the PLE signal of the GaAs fundamental absorption at approximately 1.5 eV is much weaker in the spectrum for sample A than in that for sample B. From these results, the abrupt absorption edge observed at 1.6 eV in the PLE spectrum of sample A in the as-grown state is concluded to be direct evidence of the optical absorption by the  $E_+$ -related band of the GaAs:N  $\delta$ -doped SL.

It is also assumed that the enhancement of the optical transition intensities associated with the  $E_+$  minibands in

GaAs:N  $\delta$ -doped SLs, which have been confirmed by PR, contributes to the observation of the absorption characteristics in the high-energy range. The PLE spectrum of the annealed sample, in which the periodic distribution of N is destroyed, as revealed by the XRD measurement, represents the disappearance of the strong absorption onset at 1.6 eV, as shown in Fig. 5. The disappearance of the absorption onset corroborates that the periodic distribution of N plays an important role in the formation of a SL potential related to the high-energy  $E_+$  band and the enhanced absorption due to the  $E_+$  miniband in the dilute nitride semiconductor.

In conclusion, we have investigated the optical absorption characteristics of GaAs:N  $\delta$ -doped SLs using PLE, and have successfully shown direct evidence of the strong absorption due to the  $E_+$ -related band induced by N incorporation. A clear absorption edge is observed at 1.6 eV in the PLE spectrum of the SL that is sandwiched between AlGaAs blocking layers. The absorption edge energy well corresponds to a transition energy associated with the  $E_+$  band of the SL estimated from a PR spectrum. The AlGaAs layers on both edges of the SL region block the photogenerated carriers from the GaAs regions in the sample, and thus the effect from them on the PLE measurements is suppressed, resulting in the successful detection of the absorption of the high-energy conduction subband in the dilute nitride semiconductor. The excellent absorption properties of GaAs:N  $\delta$ -doped SLs as an intermediate-band material are expected to lead to further progress in high-efficiency IBSC developments.

1) A. Luque and A. Martí, *Phys. Rev. Lett.* **78**, 5014 (1997).

2) E. Cánovas, A. Martí, A. Luque, and W. Walukiewicz, *Appl. Phys. Lett.* **93**, 174109 (2008).

- 3) N. López, L. A. Reichertz, K. M. Yu, K. Campman, and W. Walukiewicz, *Phys. Rev. Lett.* **106**, 028701 (2011).
- 4) N. Ahsan, N. Miyashita, M. M. Islam, K. M. Yu, W. Walukiewicz, and Y. Okada, *Appl. Phys. Lett.* **100**, 172111 (2012).
- 5) N. Ahsan, N. Miyashita, M. M. Islam, K. M. Yu, W. Walukiewicz, and Y. Okada, *IEEE J. Photovoltaics* **3**, 730 (2013).
- 6) W. Shan, W. Walukiewicz, J. W. Ager, III, E. E. Haller, J. F. Geisz, D. J. Friedman, J. M. Olson, and S. R. Kurtz, *Phys. Rev. Lett.* **82**, 1221 (1999).
- 7) W. Shan, W. Walukiewicz, K. M. Yu, J. W. Ager, III, E. E. Haller, J. F. Geisz, D. J. Friedman, J. M. Olson, S. R. Kurtz, and C. Nauka, *Phys. Rev. B* **62**, 4211 (2000).
- 8) M. Geddo, T. Ciabattini, G. Guizzetti, M. Patrini, A. Polimeni, R. Trotta, M. Capizzi, G. Bais, M. Piccin, S. Rubini, F. Martelli, and A. Franciosi, *Appl. Phys. Lett.* **90**, 091907 (2007).
- 9) A. Grau, T. Passow, and M. Hetterich, *Appl. Phys. Lett.* **89**, 202105 (2006).
- 10) J. D. Perkins, A. Mascarenhas, Y. Zhang, J. F. Geisz, D. J. Friedman, J. M. Olson, and S. R. Kurtz, *Phys. Rev. Lett.* **82**, 3312 (1999).
- 11) C. Skierbiszewski, P. Perlin, P. Wisniewski, T. Suski, J. F. Geisz, K. Hingerl, W. Jantsch, D. E. Mars, and W. Walukiewicz, *Phys. Rev. B* **65**, 035207 (2001).
- 12) P. Perlin, P. Wisniewski, C. Skierbiszewski, T. Suski, E. Kaminska, D. E. Mars, and W. Walukiewicz, *Appl. Phys. Lett.* **76**, 1279 (2000).
- 13) Y. Endo, K. Tanioka, Y. Hijikata, H. Yaguchi, S. Yoshida, M. Yoshita, H. Akiyama, W. Ono, F. Nakajima, R. Katayama, and K. Onabe, *J. Cryst. Growth* **298**, 73 (2007).
- 14) T. Fukushima, Y. Hijikata, H. Yaguchi, S. Yoshida, M. Okano, M. Yoshita, H. Akiyama, S. Kuboya, R. Katayama, and K. Onabe, *Physica E* **42**, 2529 (2010).
- 15) K. Takamiya, Y. Endo, T. Fukushima, S. Yagi, Y. Hijikata, T. Mochizuki, M. Yoshita, H. Akiyama, S. Kuboya, K. Onabe, R. Katayama, and H. Yaguchi, *Mater. Sci. Forum* **706–709**, 2916 (2012).
- 16) K. Takamiya, T. Fukushima, S. Yagi, Y. Hijikata, T. Mochizuki, M. Yoshita, H. Akiyama, S. Kuboya, K. Onabe, R. Katayama, and H. Yaguchi, *Appl. Phys. Express* **5**, 111201 (2012).
- 17) F. Ishikawa, S. Furuse, K. Sumiya, A. Kinoshita, and M. Morifuji, *J. Appl. Phys.* **111**, 053512 (2012).
- 18) S. Noguchi, S. Yagi, D. Sato, Y. Hijikata, K. Onabe, S. Kuboya, and H. Yaguchi, *IEEE J. Photovoltaics* **3**, 1287 (2013).
- 19) S. Yagi, S. Noguchi, Y. Hijikata, S. Kuboya, K. Onabe, and H. Yaguchi, *Jpn. J. Appl. Phys.* **52**, 102302 (2013).
- 20) D. E. Aspnes, *Surf. Sci.* **37**, 418 (1973).